Scanning Microscopy

Volume 3 | Number 2 Article 1

7-29-1989

Scanning Tunneling Microscopy of Proteins on Graphite Surfaces

L. Feng
University of Utah

J. D. Andrade
University of Utah

C. Z. Hu
University of Utah

Scanning Microscopy, Vol. 3, No. 2, 1989 (Pages 399-410) 0891-7035/89$3.00+.00
Scanning Microscopy International, Chicago (AMF O'Hare), IL 60666 USA

SCANNING TUNNELING MICROSCOPY OF PROTEINS ON GRAPHITE SURFACES

L. Feng, J.D. Andrade*, and C.Z. Hu

Department of Bioengineering & Center for Biopolymers at Interfaces
College of Engineering
University of Utah
Salt Lake City, Utah 84112
U. S. A.

(Received for publication April 09, 1989, and in revised form July 29, 1989)

Abstract

We applied scanning tunneling microscopy (STM) to the observation of amino acids and proteins deposited and/or adsorbed on highly oriented pyrolytic graphite (HOPG).

Although many questions remain, it is demonstrated that relatively high resolution images of uncoated proteins can often be obtained in air. We present images of five amino acids (glycine, leucine, lysine, methionine and tryptophan) and three proteins (lysozyme, albumin and fibrinogen) under various conditions of deposition and adsorption. We discuss the role of affinity of the amino acids and proteins to the substrate, their adsorbed states and distribution, and STM tip-induced deformation and/or destruction.

STM studies of adsorbed proteins are expected to provide useful and even unique information on the conformation and packing of the proteins.

KEY WORDS: Scanning tunneling microscopy, Biological applications, Highly oriented pyrolytic graphite, Proteins, Amino acids, Lysozyme, Albumin, Fibrinogen.

*Address for correspondence:
Department of Bioengineering
College of Engineering, University of Utah
Salt Lake City, UT 84112
U.S.A. Phone No. (801) 581-4379

Introduction

Scanning tunneling microscopy (STM) is a new and fast growing surface analysis and imaging technique. In the seven or so years since its invention by Binnig and Rohrer (Binnig et al.,1982), STM has been gradually increasing in popularity in the imaging of conducting and semi-conducting surfaces (Binnig and Rohrer,1985, Quate, 1986, and Hansma and Tersoff, 1987). Such rapid progress is due to the unparalleled capabilities of STM compared with other forms of microscopy: (1) ultra-high resolution down to atomic dimensions, (2) three-dimensional images, especially with a very high sensitivity in the vertical direction, (3) a variety of operating conditions, including vacuum, air and even liquids, (4) observation range from 10^{-6} to 10^{-10} m, (5) the ability to do tunneling spectroscopy, and (6) relatively inexpensive equipment.

The operating principle of STM is surprisingly simple. When a metal needle-like probe (tip) is brought close enough to a conducting surface (1-10 Angstroms), electrons tunnel through the gap between the tip and the surface under an appropriate bias voltage, producing a tunneling current. The tunneling current is a function of the bias voltage and the shape of the barrier (related to work function) and is extremely sensitive to the gap distance. The tunneling current is changed by a factor of 10 when the distance changes just 1 Angstrom for a local work function of 4 eV. It is this strong distance dependence that is the reason for STM's high vertical resolution. When the tip is rastered across the surface using a piezoscanner, a feedback network adjusts the height of the tip above the substrate surface to keep the tunneling current constant; this is called the constant current mode. Alternately, the change in the tunneling current can be recorded at a constant tip height: the constant height mode. In

both modes a surface topographical map is obtained (Hansma and Tersoff, 1987), as in Figure 1, if the substrate has a a chemically homogeneous surface. Suppose there is an adsorbed molecule on a conducting surface; it may perturb the magnitude of the local tunneling current due to a change in local work function. The molecule is "imaged" through the change of the local current. This is the probable mechanism by which an adsorbate is detected by STM (Panitz, 1987 and Spong et al. 1989). Since the adsorbate usually does not have the identical chemical composition and structure as the substrate, the tunneling current map does not necessarily represent the same surface topography.

Since our group has a strong involvement in the study of proteins at interfaces (Andrade, 1985), we have a particular interest in applying STM to this area. Our rationale is as follows: conventional TEM or SEM generally needs a high vacuum system, which often distorts the protein native state. Often a coating is necessary to minimize sample charging and to enhance the contrast; such coating can easily introduce artifacts and thereby decrease the useful resolution. Labeling adsorbed proteins with heavy metals, such as gold, does not give a sufficiently high resolution in the SEM, and it depends on labeling efficiency and other factors. However, with an in-air-operated STM it is possible to observe proteins in their hydrated state in a humid environment.It is even possible to see proteins in solution with an appropriately designed and constructed STM. Proteins are considered semiconductive in their usual hydrated state (Jortner and Bixon, 1987). The resolution of STM for protein molecules should be higher than in SEM or TEM. So long as the substrate conducts electricity, STM may be employed.

A brief review of STM applications in biology

Listed here are the major obstacles in applying STM to the study of proteins. (1) They are, in general, poor conductors of electricity so that they may not significantly alter the tunneling current; (2) they are relatively soft and flexible so that they tend to "smear out" the image and lower the resolution because of their motion and relaxation in the presence of the tip and the applied electric field; (3) their molecular structure is often not well characterized so that image interpretation is difficult; and (4) they may have weak interactions with the conducting substrate to which they are attached so that they are often perturbed or moved by the moving tip. Nevertheless, many biological as well as organic substances in different forms have been observed by STM. A few review papers are now available (Hansma et al., 1988 and Zasadzinski, 1989).

The very first paper of STM images of a biological substance, DNA, appeared in 1983 (Binnig and Rohrer, 1983), unveiling the possible application of STM in biology. Baro et al. (1985,1986) reported the surface topography of bacteriophage f29 on graphite There have been a number of papers on imaging Langmuir-Blodgett films on different substrates by STM, with arachidate on graphite (Smith et al., 1987), dimyristoylphosphatic acid on both

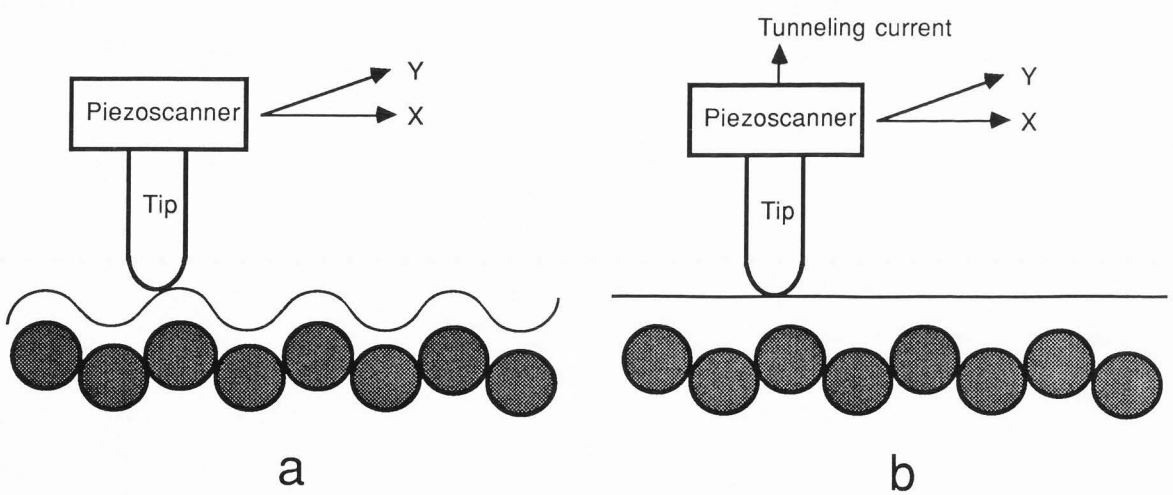

Figure 1. Schematic expression of operating principles of scanning tunneling microscopy in either the constant current mode and constant height mode.

graphite and gold (Horber et al., 1988), o-tricosenoic and 12,8-diynoic acids (Cd salts) on silicon wafer and graphite (Braun et al., 1988). It seems that with such regularly packed structures, the molecules are much easier to image and distinguish and the resolution is higher compared to individual or randomly packed molecules. The same is true when imaging liquid crystals (Foster and Frommer, 1988 and Spong et al., 1989) and TTF-TCNQ crystals (Sleator and Tycko, 1988). Stemmer et al. (1987) have managed to image biological membranes (porin membrane). Membranes prepared by freeze-fracture replica methods show much more detail (Joseph et al., 1988). Studies of single stranded DNA have produced impressive results. Travaglini et al. (1987) started the study of bare DNA molecules. Later the same group obtained images of DNA by means of conducting film coatings (Amrein et al., 1988). Beebe et al.(1989) achieved a similar resolution on uncoated double-stranded DNA using STM. DNA images under water were obtained by Barris et al.(1988) and Lindsay et al.(1989).

Few papers have dealt with the subject of STM observation of proteins. One of the earliest papers on protein STM images was by Dahn et al.(1988). While their work was mainly on bacterial sheaths, a globular protein, ovalbumin, was imaged. The molecules had become flattened and elongated presumably due to the dehydration. Horber et al. (1988) studied Concanavalin A embedded in a lipid film. They claimed that the four subunits of Con A might be seen. Simic'-Krstic' et al. (1989) recently observed microtubules on graphite fixed in 0.1% glutaraldehyde in both freeze dried and hydrated states. Microtubules frequently appeared buckled, semiflattened and/or twisted. Collagen strands of 15 Angstroms in diameter on graphite were imaged by Voelker et al.(1988). They suggested that the periodic spikes from the strand represented pyrrolidine rings of the proline and hydroxyproline amino acid residues. In contrast to the DNA images, proteins on a conducting substrate generally show a less defined structure and poorer resolution.

Since protein adsorption properties play an important role in the applications of biomaterials, we believe that it is worthwhile to utilize STM to explore the details in conformation and packing of adsorbed proteins. STM may also provide information on the electronic structure of proteins which will certainly benefit molecular electronics studies. In the rest of the paper, we will introduce our published and unpublished STM work on five amino acids and three proteins (Feng et al., 1988 and 1989).

Experiments

The substrate was highly oriented pyrolytic graphite (HOPG) from Union Carbide. As a routine substrate for STM, HOPG is a semimetal and relatively inert material. Cleaved by an adhesive tape, HOPG readily provides a large (1 mm x 1 mm) clean area with an atomically flat plane. Tryptophan (trp) was from Calbiochem and glycine (gly), leucine (leu), lysine (lys), and methionine (met) were from Sigma. Hen lysozyme was from Calbiochem, human serum albumin from Calbiochem and human fibrinogen from Calbiochem and Sigma. The amino acids and proteins were dissolved either in ultra-pure water (10 MΩ/cm) or in pH 7.4 phosphate buffered saline (PBS); amino acid concentrations were 0.1 mg/ml and protein concentrations were from 0.001 mg/ml (1 ppm) to 0.1 mg/ml (100 ppm). A droplet of the solution was pipetted onto a newly cleaved HOPG surface, which was either promptly removed by capillarity (for a deposited sample) or allowed to rest for 5 min before being flushed with ultra-pure water (for an adsorbed sample). All samples were dried at room temperature and ambient atmosphere (22°C and 20-50% R.H.).

Our STM was provided by the Tunneling Microscope Co.(Smith, 1987). STM tips were prepared by electrochemical etching a tungsten wire, 0.5 mm in diameter, in a 2 M KOH solution under a 20-30 V a. c. potential. The tips had diameters from 0.1-1 mm at the end as measured by TEM. STM was operated in air; both constant height and constant current modes were used. Parameters for a typical constant height mode were 200-800 mV bias voltage (Vb), tips being negative with respect to samples, 1-2 nA tunneling current (It), 1 KHz scan rate in x direction and 1 Hz in y direction. Parameters for a typical constant current mode were 50-400 mV bias voltage, tips being negative with respect to samples, 1-4 nA tunneling current, 30 Hz scan rate in x direction and 0.05 Hz in y direction. The magnification was calibrated by the lattice parameters of HOPG substrate. Real-time images were processed by a band pass filter to minimize high frequency noise, and displayed by an oscilloscope. The pictures were recorded from the oscilloscope by a CRT camera.

Results and discussion

Amino acids (Feng et al., 1988)

We first studied the amino acids since they are the simpler building blocks of complex proteins. All five amino acids adsorbed on HOPG were easily seen as aggregates (Figure 2). Adsorbates occupied roughly 5-10% of

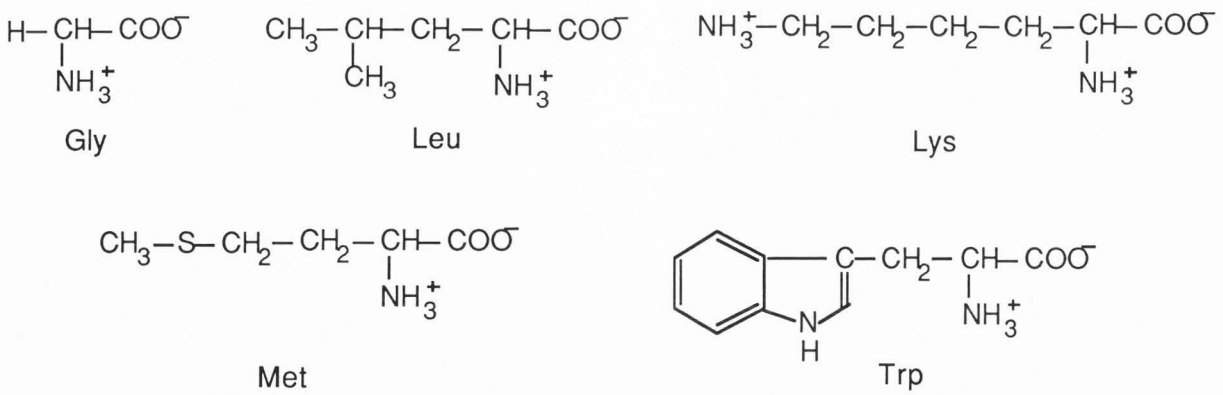

a

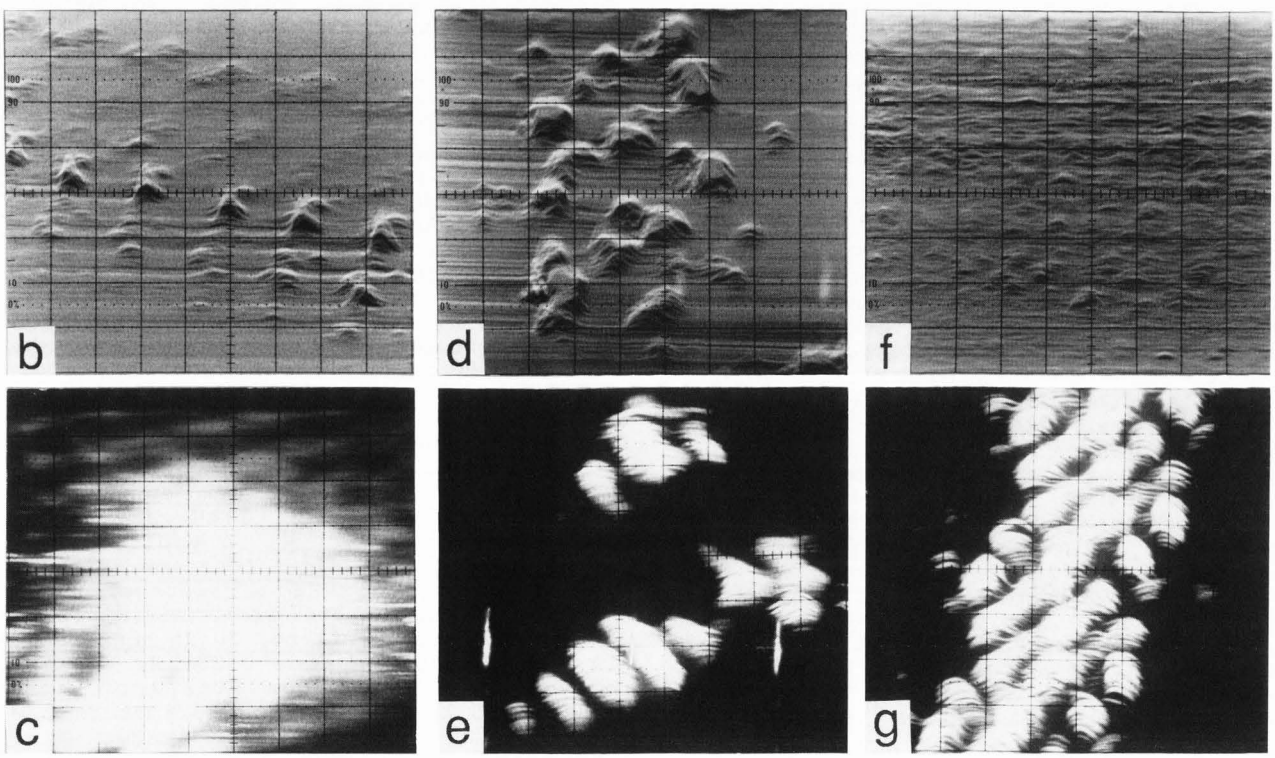

Figure 2. (a) Molecular formulas of the five amino acids. (b) - (g) Amino acids adsorbed from 0.1 mg/ml aqueous solutions on HOPG as aggregates: (b) Gly (Vb = 500 mV, It = 1 nA, 25 Angstroms/div): (c) One of the humps in (b), 2.5 Angstroms/div; (d) Lys (Vb = 300 mV, It = 1 nA, 25 Angstroms/div); the white vertical lines are photo defects; (e) Higher magnification of (d), 2.5 Angstroms/div; the white vertical lines are photo defects; (f) Met (Vb =800 mV, It = 1 nA, 25 Angstroms/div); (g) Higher magnification of met (Vb = 300 mV, It = 1.8 nA, 2.5 Angstroms/div). In (c), (e) and (g), individual molecules can be barely seen. Constant height mode was used.

total surface, according to a statistical estimate with many regions. This value is much less than that expected from our radioisotope measurements, which gave about 80% coverage if monolayer adsorption was assumed. The discrepancy may be due to: (1) the presence of multilayer adsorbates which had been truncated by the STM tip because the gap distance was of the order of 1 Angstrom, (2) loss of adsorbates from the substrate when they were impounded by the rigid tip, and/or (3) incapability of imaging some adsorbates since they did not modify the tunneling current. From Figures 2 (c), (e) and (g) one could distinguish a few single molecules in those clusters. The apparent difference in their sizes is thought due to their different distances to the tip since they were randomly packed. More often than not, separate individual amino acid molecules were hard to find, presumably due to weak interactions between them and the substrate. Sometimes a molecule was spotted but it quickly disappeared from the image before a picture could be taken.

Occasionally, a few amino acid molecules were caught and imaged with better resolution, as in Figure 3. We suggest that the bright humps represent amino acid molecules because: (1) the dimensions of the three species, estimated with reference to the graphite crystal lattice, agree with those expected from the molecular models (see the insertions in each figure); (2) "bright humps" were frequently observed for the adsorbed samples but similar images were not seen on clean HOPG surfaces or on a control sample which had undergone identical sample preparation procedures except for no amino acids; (3) taking pictures of the bright humps turned out to be difficult since they tended to escape very easily due to their weak interactions with the substrate; (4) adsorption from the atmosphere was not given strong consideration because graphite surface images were routinely obtained on "clean" HOPG, even samples used several days after cleavage; (5) hydrocarbon impurities, if any, are not normally seen by STM, Schneir and Hansma(1987); and (6) all the pictures in this paper are representatives of many observation events. Dimers or trimers are relatively more stable than monomers in terms of interactions with the substrate so that they were immobile for a sufficient time for producing a photograph. No dimers or even trimers could be seen on gly samples because of gly's much smaller molecular weight and size.

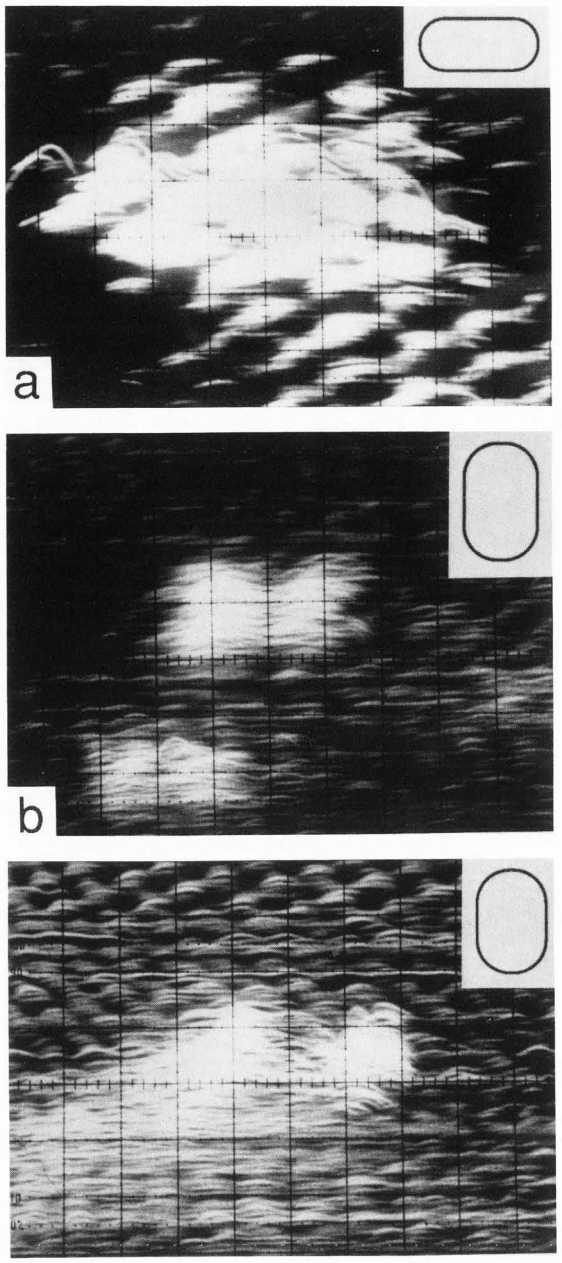

Figure 3. Images of individual amino acid molecules with constant height mode. The graphite substrate can be seen underneath. The insertions are the molecular sizes based on CPK models of the same magnification as the images. (a) Gly image (1.9 Angstroms/div in x and 3.2 Angstroms/div in y), a number of gly molecules apparently pack together; (b) Leu image (2.8 Angstroms/div in x and 3.2 Angstroms/div in y), three leu molecules being seen, two of which are associated to form a dimer; (c) Trp image (3.3 Angstroms/div in x and 3.8 Angstroms/div in y), a dimer of two parallel packed molecules being seen.

Hen egg-white lysozyme

Hen egg-white lysozyme is a small compact protein with molecular weight of 14,600, made up of a single polypeptide chain of 129 amino acids. Four disulfide bonds cross-link the molecule and provide high stability. Lysozyme has an ellipsoidal shape, with dimension of 45 x 30 x 30 Angstroms (Stryer, 1988). ESCA measurement, Figure 4, shows that lysozyme has a large affinity for HOPG. The adsorbed monolayer (the plateau of the adsorption isotherm) was formed within 5 min even when the solution concentration was as low as 0.01 mg/ml, and virtually no desorption was detected.

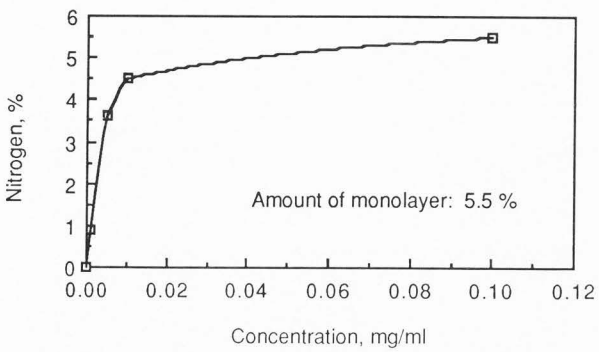

Figure 4. Lysozyme adsorption isotherm detected by ESCA (HP 5958C); adsorption time 5 min at 22°C, and water rinse 1 min.

In Figure 5(a), adsorbed lysozyme is observed by the constant height mode. The molecules apparently collapsed and merged into a rough film. The adsorbate film was apparently thin enough to have avoided being cut through by the STM tip. A very small number of molecules remained roughly of globular shape (Figure 5(b)). But this time their top portions were apparently truncated by the tip. In order to image the whole molecule, the constant current mode should be a better method for molecules with dimensions of more than several Angstroms.

Figure 6 is the image using the constant current mode. Again no individual molecules are recognizable even with higher magnification. Compared with Figure 5(a), this picture shows much rough adsorbates with many "hills" and "valleys". One of the reasons might be that the constant current mode tolerated much larger sized objects since the tip tried to go over them. Another possible reason is that the tip tended to mechanically push the molecules and piled them up if they did not enhance the

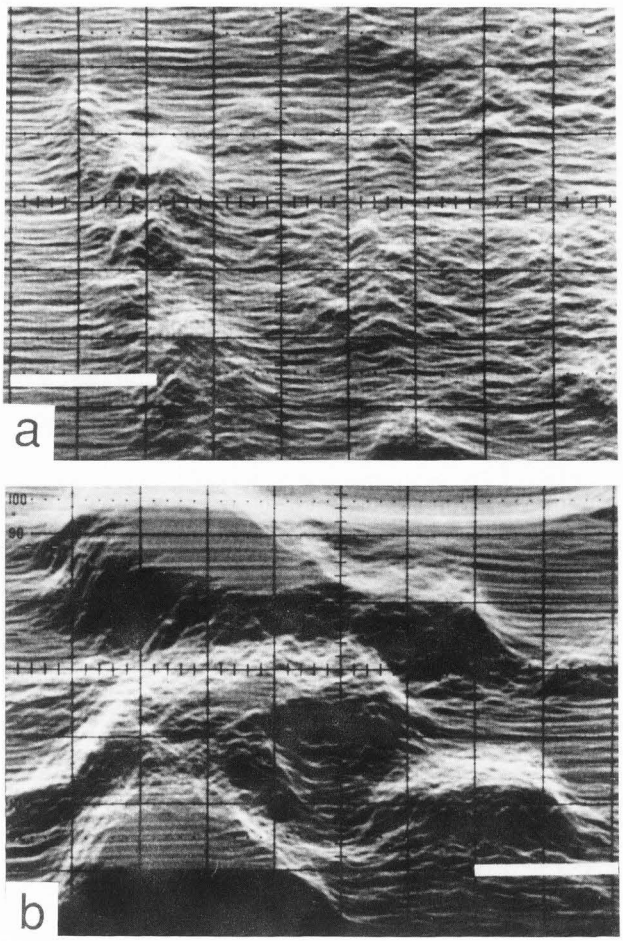

Figure 5. STM images of adsorbed lysozyme on HOPG, adsorption conditions: 0.1 mg/ml concentration, adsorption time 5 min at 22°C, and water rinse 1 min; STM conditions: constant height mode, Vb = 800 mV, It = 2 nA. (a) Most lysozyme molecules merged into a rough adsorbed layer, bar = 40 Angstroms. (b) In very few cases globular molecules remained but their top portions were apparently truncated by the tip, bar = 40 Angstroms.

tunneling current sufficiently to provide response in the gap distance adjustment. The latter perhaps dominated since lysozyme molecules had high resistivity and therefore were hardly "seen" by the tip.

Human serum albumin (Feng et al., 1988)

Human serum albumin consists of a single polypeptide chain of 584 amino acids with a molecular weight of about 69,000. Albumin has a strong internal structure, held firmly together by seventeen disulfide bridges. Figure 7

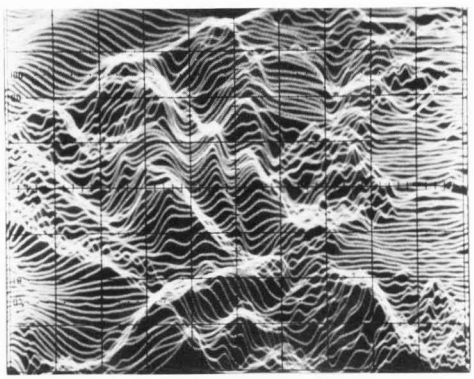

Figure 6. STM images (100 Angstroms/div) of adsorbed lysozyme on HOPG, adsorption conditions: 0.1 mg/ml concentration, adsorption time 5 min at 22°C, and water rinse 1 min; STM conditions: constant current mode, Vb = 300 mV, It = 1.8 nA.

shows the three-dimensional molecular model (Brown and Shockley, 1982). The molecular shape is generally taken as an ellipsoid with dimensions of 40 x 140 Angstroms. There are three domains within the molecule. The domain structure is believed to be a cylinder formed by six a-helices. This structure has now been partially confirmed by the recent x-ray crystal structure analysis (Carter et al., 1989).

The STM images of human albumin are presented in Figure 8 although they have been difficult to repeat. Figure 8(a) shows one adsorbed human albumin molecule and some parts of two other molecules on HOPG. They have different orientations. The molecular dimensions are 120 Angstroms in length and 60 Angstroms in width. The slight deviation in dimensions of the adsorbate from those of the above model may be caused by slight collapse of the native structure in the relatively dry air environment. Three cylindrical, parallel domains can be observed, as expected from the model, suggesting that the surface denaturation may not be extensive. In addition to domains, some side loops connecting the domains can also be seen. The fact that domains can be distinguished means that the resolution is about 10 Angstroms. The flat regions around the adsorbed molecules have been identified as bare HOPG. In fact, the tiny ripples along the scanning lines in Figure 8(b) are the corrugation of graphitic carbon atoms, commonly observed by STM on HOPG. The surface depression to the left of each adsorbed molecule is due to the delayed time response of the tip, which was scanning from right to left. Figure 8 gives information on adsorption as well. The albumin molecules essentially maintained a nearly native state in the presence of interactions between the adsorbate and the adsorbent. There has been little apparent denaturation.

Human fibrinogen

The importance of fibrinogen adsorption to the understanding of the blood-compatibility of materials and the molecule's unique three-nodular structure lured us to observe it with STM. Fibrinogen is a big protein with molecular weight of 341,000. From the molecular model in Figure 9(a), we see that its dimensions are approximately 450 Angstroms in length and 65 Angstroms in diameter (Williams, 1981). Although we never succeeded in imaging an intact fibrinogen molecule, it turned out that we have ended up with much more information about STM itself.

Figure 9(b) displays a typical fibrinogen molecule, which looks like a "slab". Referring to Figure 9(a), one realizes that the macromolecule observed

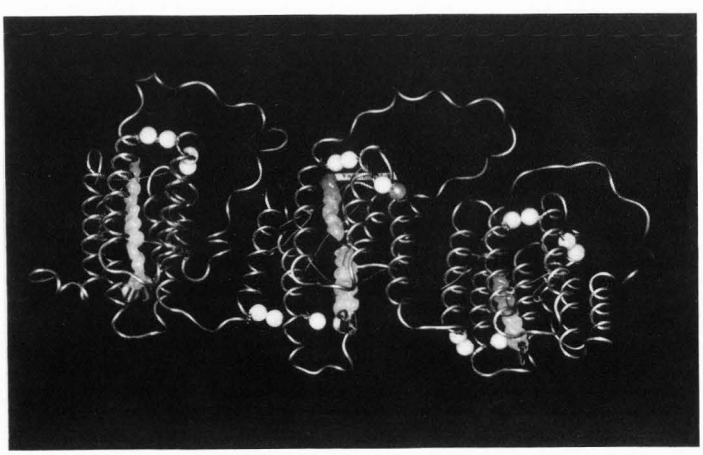

Figure 7. Backbone 3 dimensional model of serum albumin. In this model the wire represents the peptide backbone and the spheres represent disulfide bridges in the long loops. The three domains are antiparallel to one another. The length is 140 Angstroms and the width 40 Angstroms for the entire molecule (from Brown and Shockley, 1982 by permission of the author). See reference.

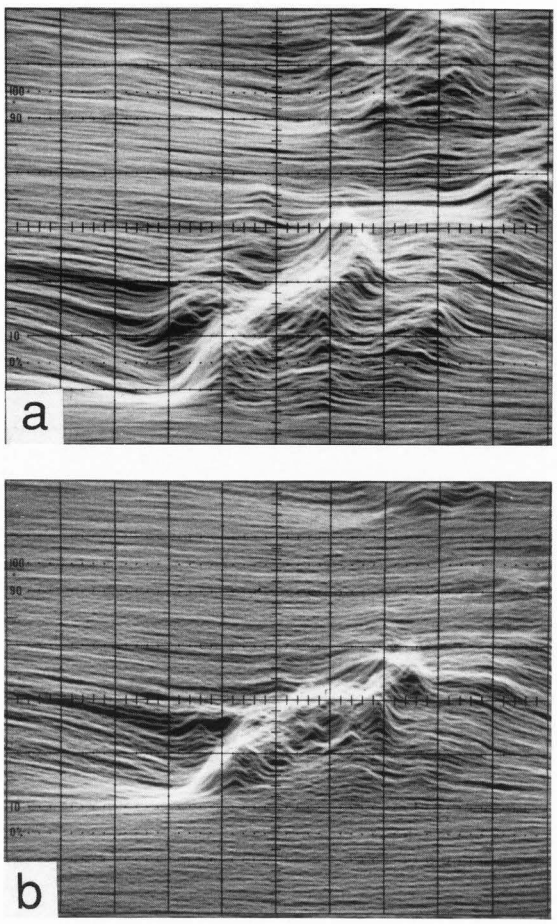

Figure 8. Images of human albumin on HOPG. The picture dimensions are 200 Angstroms in the horizontal (x) and 160 Angstroms in the vertical (y) directions. Since the adsorbate has a very different electronic structure from the substrate, the height (z direction) could not be directly measured. Both (a) and (b) show several different molecules. Three domains can be clearly seen (a). The ripples on the raster lines in (b) are the corrugations of carbon atoms of the HOPG. The sample was prepared by depositing a droplet of albumin PBS solution (10 ppm albumin) onto freshly cleaved HOPG and then the droplet was removed by capillarity with a tissue. The sample was then flushed with water for 10 sec and was dried at room temperature for 5 h before observation. The STM was operated at a bias voltage of 200 mV, tunneling current of 4 nA and high feedback gain. The constant current mode was used.

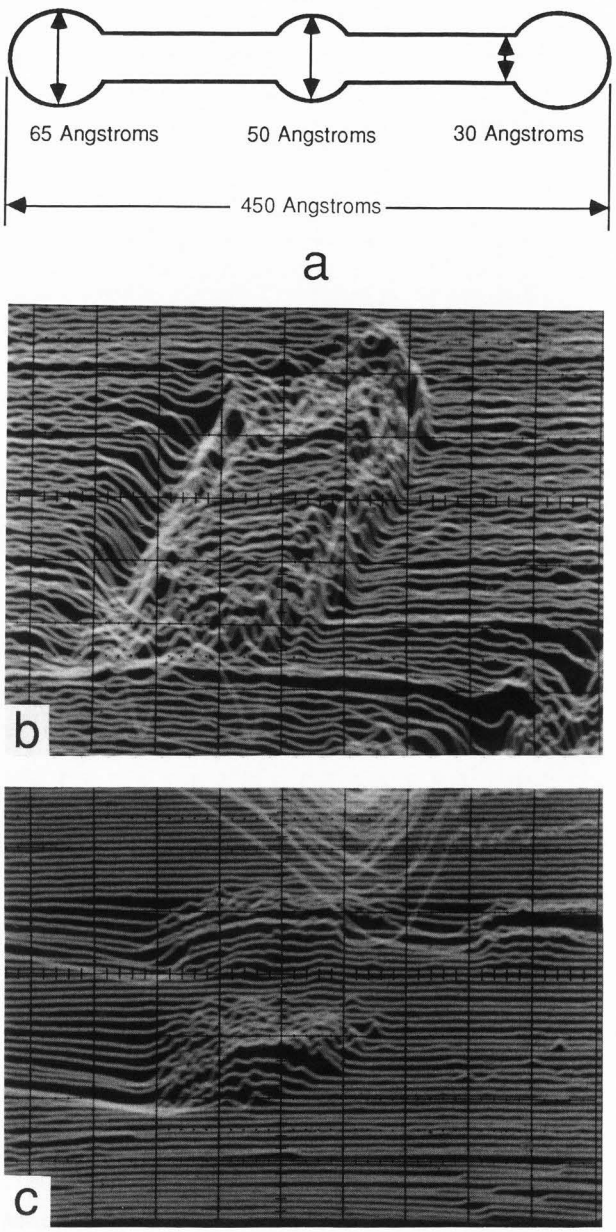

Figure 9. (a) A fibrinogen molecular model from Williams (1981); the globular domains at both ends may be elongated (90 x 40 Angstroms). (b) A typical fibrinogen molecule observed by STM on HOPG (deposited from a 20 ppm aqueous solution), constant current, Vb = 200 mV, It = 1 nA, 100 Angstroms/div. (c) An image of 3 separated domains of a fibrinogen molecule which originally was a similar slab as the one in (a), constant current, Vb = 200 mV, It = 1.5 nA, 100 Angstroms/div. The picture was taken when the trace of water on the sample just disappeared.

in Figure 9(b) had been so severely deformed that it had lost its key characteristics. While its length remained relatively unchanged its width expanded to 400 from 65 Angstroms and its height was reduced to about 15 from 65 Angstroms. The more miserable thing is that it did not show the three domain structure. From the deviation of the molecular dimensions, it is reasonable to suppose that the tip had heavily squeezed, depressed, and thus distorted the fibrinogen molecule. Although fibrinogen has a large molecular size, it appears to not sufficiently increase the tunneling current. Thus, the tip could not discern this huge molecule because it judged the surface morphology by sensing the local tunneling current rather than atomic or molecular topography. Note Figure 9(c): the picture started with a "slab" at the center. A moment later the "slab" suddenly burst into three "caps", probably representing the three deformed node-like domains. This could occur because this sample was just barely dried so the molecule was softer and less adhered and/or denatured. The linking chains between the domains had apparently been fractured such that the domains were no longer in an axis but rather randomly scattered.

The "slabs" certainly were not part of the substrate, as might be suggested, since they were quite mobile on the substrate. The whole process is illustrated in Figure 10. A single molecule did not have sufficient interaction with the substrate HOPG to immobilize itself. As we mentioned before, owing to some degree of mechanical contact, the tip was driving fibrinogen molecules around and they kept moving until many of them packed together, which increased their mutual interaction. This sort of dynamic process was observed with several different samples.

Although a few individual molecules were imaged, the majority of the STM images showed aggregates of fibrinogen molecules, as in Figure 11, in which the lower left hand flat region was the HOPG substrate. In spite of our attempt to create the conditions favoring the formation of separate molecules, their distribution seems to have nothing to do with the methods of preparation of

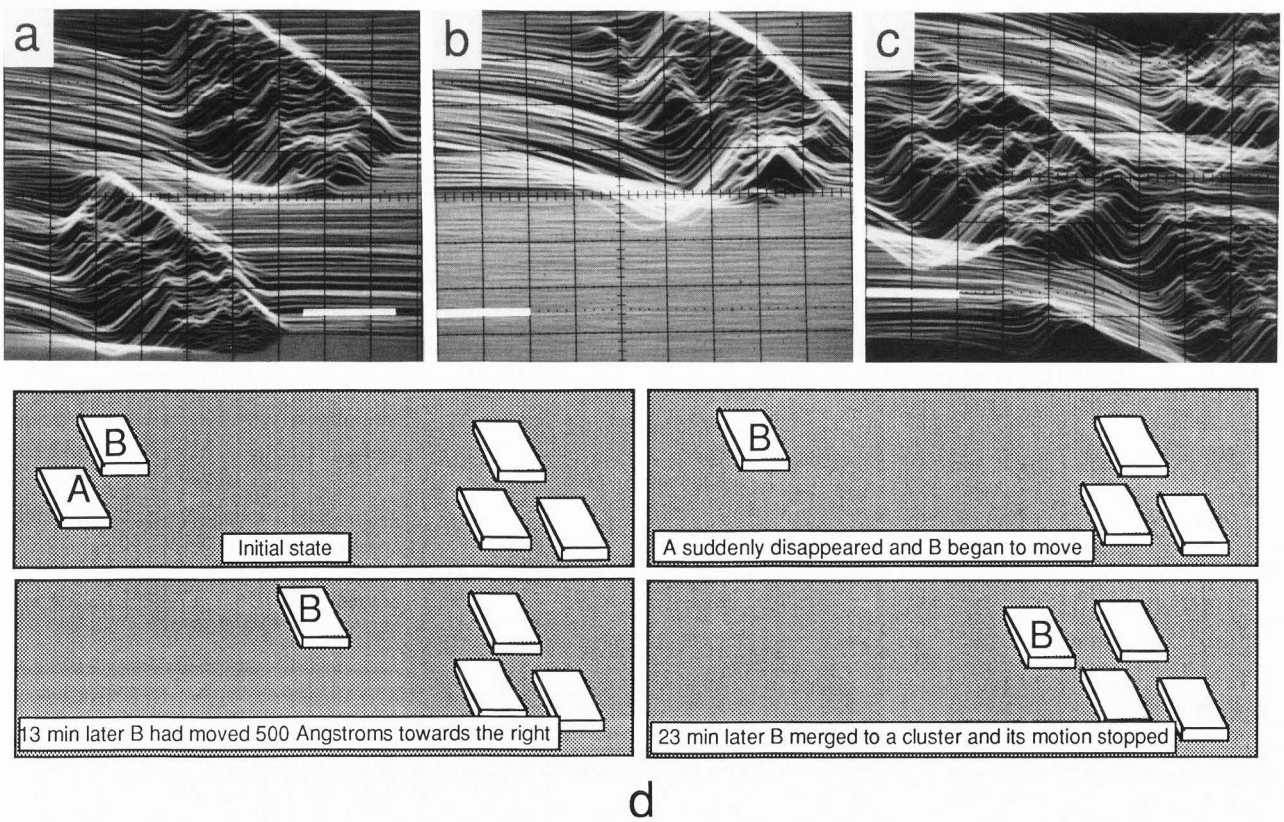

Figure 10. A dynamic process of fibrinogen molecules on HOPG, constant current, Vb = 200 mV, It = 3 nA, 100 Angstroms/div. (a)-(c) recorded the motion and (d) illustrates the entire process.

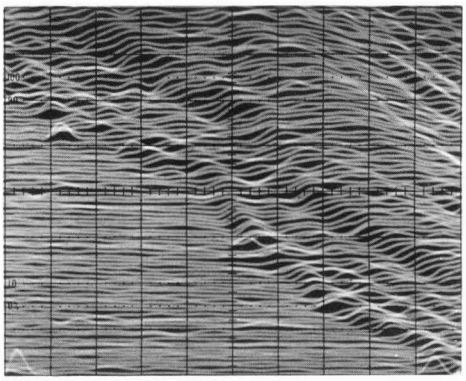

Figure 11. An edge of adsorbed fibrinogen aggregate, whose area was larger than 1 x 1 mm. The lower left handed flat region was the HOPG substrate (Deposited from a 5 ppm PBS solution, constant current, Vb = 800 mV, It = 2 nA, 100 Angstroms/div).

---

samples, be it deposit or adsorption, whether or not water flushed, and high or low concentrations of the solutions. Just as in the lysozyme case, it is suspected that the tip had driven and piled up segregated molecules into clusters. But this time we have more confidence in this suggestion, since we have evidence of such a dynamic process.

Remarks

Although there is no doubt that protein molecules can be observed on a conducting substrate by STM, depending on various circumstances, the difficulty is how to observe them without altering their initial adsorbed state, how to reproducibly obtain similar images, and under what conditions an adsorbed protein molecule can be unambiguously observed. A number of important questions have to be answered: What is the mechanism of image formation of such poorly conductive substances? What role do the tip geometry and surface chemistry play? What is the major interaction between the tip and a protein molecule: mechanical or electronic? What effects does the conducting substrate impose, such as its deformation, electron density, etc? What is the role of sample hydration or water sorption? We are continuing to address these questions.

Conclusions

Our STM work on proteins adsorbed on HOPG can be summarized as follows:

(1) Both amino acids and proteins can be seen by STM under certain conditions despite some difficulties.

(2) Amino acids are adsorbed both as aggregates and as individual molecules. Single molecules are apt to escape under the STM tip since their interactions with the substrate are weak.

(3) Hen egg-white lysozyme undergoes a conformational change upon adsorption and/or STM visualization.

(4) The high resolution images of human albumin show great promise for STM applications to protein adsorption.

(5) The STM tip may deform human fibrinogen due to mechanical contact, because of its large molecular size and poor conductivity.

(6) Fibrinogen molecules can move over the substrate, driven by the tip, causing them to pile up into clusters.

Acknowledgements

We thank Dr. A. Moore, the Union Carbide Corp., for a gift of HOPG. We especially thank Dr. C. Quate, Stanford U., for stimulating our interest and aiding our STM work on proteins. The images of lysozyme obtained in Quate's Lab in February, 1987 (unpublished) encouraged us to apply STM to the study of adsorbed proteins.

The Center for Biopolymers at Interfaces, a state of Utah Center of Excellence, supported the work. Partial support was also provided by the Office of Naval Research (ONR) contract N00014-88-0415 (W. Bascom, P. I.).

References

Amrein M, Stasiak A, Gross H, Stoll E, Travaglini G (1988) Scanning tunneling microscopy of recA-DNA complexes coated with a conducting film *Science* 240, 514-516.

Andrade JD (1985) Principles of protein adsorption. In: *Surface and Interfacial Aspects of Biomedical Polymers*. Vol. 2, Plenum, New York, pp. 1-80.

Baro AM, Miranda R, Alaman J, Garcia N, Binnig G, Rohrer H, Gerber Ch, Carracosa JL (1985) Determination of surface topography of biological specimens at high resolution by scanning tunneling microscopy *Nature* 315, 253-254.

Baro AM, Miranda R, Carrascosa JL (1986) Application to biology and technology of the scanning tunneling microscope operated in air at ambient pressure *IBM J. Res. Development* 30, 380-386.

Barris B, Knipping U, Lindsay SM, Nagahara L, Thundat T (1988) Images of DNA fragments in an aqueous environment by scanning tunneling microscopy *Biopolymers* 27, 1691-1696.

Beebe TP, Wilson TE, Ogletree DF,

Katz JE, Balhorn RB, Salmeron MB, Siekhaus WJ (1989) Direct observation of native DNA structures with the scanning tunneling microscope *Science* 243, 370-372.

Binnig G, Rohrer H (1983) Scanning tunneling microscopy. In: *Trends in Physics*. Janta J and Panatoflicek (eds.), European Physical Society, Petit-Lancy, Switzerland, pp.38-46.

Binnig G, Rohrer H (1985) The scanning tunneling microscope *Scientific American* 253, 50-56.

Binnig G, Rohrer H, Gerber Ch, Weibel E (1982) Surface studies by scanning tunneling microscopy *Phys. Rev. Lett.* 49,57-61.

Braun HG, Fuchs H, Schrepp W (1988) Surface structure investigation of Langmiur-Blodgett films *Thin Solid Films* 159, 301-314.

Brown JR, Shockley P (1982) Serum albumin: structure and characterization of its ligand binding sites. In: *Lipid-protein interactions*. Jost PC, Griffith OH (eds.), Vol. 1, Wiley, New York, pp. 25-68.

Carter DC, He XM, Munson SH, Twigg PD, Gernert KM, Broom MB, Miller TY (1989) Three-dimensional structure of human serum albumin *Science*, 244, 1195-1198.

Dahn DC, Watanabe MO, Blackford BL, Jericho MH, Beveridge TH (1988) STM imaging of biological structures *J. Vac. Sci. Technol. A* 6, 548-552.

Feng L, Hu CZ, Andrade JD (1989) Scanning tunneling microscopic images of amino acids *J. Microscopy* 152, 811-816.

Feng L, Hu CZ, Andrade JD (1988) Scanning tunneling microscopic images of adsorbed serum albumin on highly oriented pyrolytic graphite *J. Colloid Interface Sci.* 126, 650-653.

Foster JS, Frommer JE (1988) Imaging of liquid crystals using a tunneling microscope *Nature* 333, 542-545.

Hansma PK, Tersoff J (1987) Scanning tunneling microscopy *J. Appl. Phys.* 61, R1-R23.

Hansma PK, Elings VB, Marti O, Bracker CE (1988) Scanning tunneling microscopy and atomic force microscopy: application to biology and technology *Science* 242, 209-216.

Horber JKH, Lang CA, Hansch TW, Heckl WM, Mohwald H (1988) Scanning tunneling microscopy of lipid films and embedded biomolecules *Chem. Phys. Lett.* 145, 151-158.

Jortner J, Bixon M(1987) Charge exchange between localized sites. In: *Protein Structure*. Austin R (ed.), Springer-Verlag, New York, pp. 277-308.

Joseph AN, Zasadzinski J, Schneir J, Gurley J, Elings V, Hansma PK (1988) Scanning tunneling microscopy of freeze-fracture replicas of biomembranes *Science* 239, 1013-1015.

Lindsay SM, Thundat T, Lagahara L, Knipping U, Rill RL (1989) Images of the DNA double helix in water *Science* 244, 1063-1064.

Panitz JA (1987) Electron tunneling used as a probe of protein adsorption at interfaces. In: *Proteins at interfaces*. Brash J and Horbett T (eds.), Amer. Chem. Soc., Washington, DC, pp. 423-433.

Quate CF (1986) Vacuum tunneling: a new technique for microscopy *Phys. Today* Aug., 26-33.

Schneir J, Hansma PK (1987) Scanning tunneling microscopy and lithography of solid surfaces covered with nonpolar liquids *Langmuir* 3, 1025-1027.

Simic'-Krstic' Y, Kelley M, Schneiker C, Krasovich M, McCuskey R, Koruga D, Hameroff S (1989) Scanning tunneling microscopy (STM) of microtubules *FASEB Journal*, in press.

Sleator T, Tycko R (1988) Observation of individual organic molecules at a crystal surface with use of a scanning tunneling microscope *Phys Rev. Lett.* 60, 1418-1421.

Smith DPE, Bryant A, Quate CF, Rabe JP, Gerber Ch, Swalen JD (1987) Images of a lipid bilayer at molecular resolution by scanning tunneling microscopy *Proc. Natl. Acad. Sci. USA* 84, 969-972.

Smith DPE (1987) New applications of scanning tunneling microscopy Ph D dissertation, Stanford University, Stanford, CA.

Spong JK, Mizes HA, LaComb LJ, Dovek MM, Frommer JE, Foster JS (1989) Contrast mechanism for resolving organic molecules with tunneling microscopy *Nature* 338, 137-139.

Stemmer A, Rechelt R, Engel A, Rosenbusch JR, Ringger M, Hidber HR, Guntherodt HJ (1987) Scanning tunneling and scanning transmission electron microscopy of biological membranes *Surface Sci.* 181, 394-402.

Stryer L (1988) In: *Biochemistry*. 3rd edition, Freeman, New York, p. 203.

Travaglini G, Rohrer H, Amrein M, Gross H (1987) Scanning tunneling microscopy on biological matter *Surface Sci.* 181, 380-390.

Voelker MA, Hameroff SR, He JD, Dereniak EL, McCuskey RS, Schneiker CW, Chvapil TA, Bell TS, Weiss LB (1988) STM imaging of molecular collagen and phospholipid membranes *J. Microscopy* 152, 557-566.

Williams RC (1981) Morphology of bovine fibrinogen monomers and fibrin oligomers *J. Mol. Biol.* 150, 399.

Zasadzinski JAN (1989) Scanning

tunneling microscopy with applications to biological surfaces. *BioTechniques* 7, 174-187.

Discussion with Reviewers

A Aviram: Can you give a possible explanation of the conduction mechanism of the studied proteins?

Authors: At the present time, there is no general theory which can explain the contract mechanism of STM images of poorly- or even non-conductive adsorbates. Several hypotheses have been suggested, however, for some particular cases. For example: a) sorbed water may play a role in enhancing the tunneling current; b) near the Fermi level there are some empty states which can relay electrons; c) adsorbates may change the work function of the substrate underneath so that the local environment is different, etc. We did notice the effect of humidity upon the imaging of amino acids and proteins as more of these molecules could be observed in a relatively humid environment than a dry one.